

Case study

An integrated diagnostic approach to Max Ernst's painting materials in his *Attirement of the Bride*

Martina [Zuena](#)^{a,*}

martina.zuena@icmate.cnr.it

Luciano Pensabene [Buemi](#)^b

lpensabene@guggenheim-venice.it

Lena [Stringari](#)^c

lstringari@guggenheim.org

Stefano [Legnaioli](#)^d

stefano.legnaioli@cnr.it

Giulia [Lorenzetti](#)^d

a_lorenzetti@hotmail.com

Vincenzo [Palleschi](#)^d

vincenzo.palleschi@cnr.it

Luca [Nodari](#)^a

luca.nodari@cnr.it

Patrizia [Tomasin](#)^a

patrizia.tomasin@cnr.it

^aCNR-ICMATE, Corso Stati Uniti 4, 35127 Padova, Italy

^bPeggy Guggenheim Collection, 30123 Venice, Italy

^cSolomon R. Guggenheim Museum, 1071 5th Ave, 10128 New York, USA

^dCNR-ICCOM, Via G. Moruzzi 1, 56124 Pisa, Italy

*Corresponding author at: CNR-ICMATE, Corso Stati Uniti 4, 35127 Padova, Italy.

Abstract

The *Attirement of the Bride*, painted by Max Ernst in 1940, is permanently on display in the Peggy Guggenheim Collection (PGC) in Venice. Within the framework of a larger study of materials and techniques of works by Ernst at the PGC, researchers carried out a series of non-invasive analyses. A combined approach based on Vis-NIR multispectral imaging, Raman Spectroscopy, X-Ray Fluorescence (XRF), and External Reflection Fourier Transform Infrared Spectroscopy (ER-FTIR), was conducted *in-situ* in the museum galleries. In addition, two micro-samples were analysed with SEM-EDS and μ -Raman. This approach produced vital information on the preparatory drawing, the *pentimenti*, the pigments, the extenders and the alteration products present in the painting. The results showed also the presence of a white preparatory layer, under the pictorial one and above the canvas, composed by lithopone (a mixture of zinc sulphide and barium sulphate), basic lead carbonate and calcium carbonate. The latter compound is probably present also as an extender. The palette included both traditional and new synthetic, commercial pigments, used as primary colours or in mixtures. Moreover, in several areas of the painting, zinc oxalates have been identified as alteration products and more rarely, zinc metal soaps, which could also be present as additives in the paint tube. These analyses revealed the masterful and innovative painting technique of this pioneer of Surrealism.

Keywords: Oil painting; Multispectral imaging; ER-FTIR; XRF; Raman spectroscopy; SEM-EDS

1 Research aim

The aim of this study is to provide a characterization of the painting materials used by the German artist Max Ernst, whose painting technique has never been widely investigated from a scientific point of view. He worked in a transition period where the use of new synthetic materials increased with respect to the traditional ones. The purpose of the research was achieved by studying an oil painting exposed to the Peggy Guggenheim collection in Venice through a multi-analytical approach. It mostly involved non-invasive technique, adopted directly *in situ*. However, there was also the possibility to analyse two micro-samples in laboratory. The combined results obtained from each single analysis provided valuable information for a better understanding of the artist's painting technique.

2 Introduction

Conservation of 20th century paintings presents challenges for scientists and conservators, given a plethora of new industrial and synthetic materials whose response to environmental conditions and evolution over time are still not well known [1-3]. Modern art has not been as thoroughly investigated as more traditional and historical painting techniques. New paint recipes, in particular commercial oil paint formulations, include a variety of relatively unexplored pigments and dyes, drying oils, fillers, extenders and stabilizers [4-6]. Therefore, the characterization of the materials is crucial to first understand the choices of the artist and secondly, to determine suitable environmental conditions for the display and storage of the works as well as to develop a conservation strategy when needed. In particular, the integration of data deriving from a multi-analytical approach is very useful to overcome the limitations of each single analysis, thus providing more definite information about constituent materials and painting techniques. Among the possible methodologies, the non-invasive ones applied directly *in situ* are usually preferred as providing valuable information while preserving the integrity of the artworks [7-11].

Within the framework of a larger collaborative project between the Italian National Research Council (CNR) and the Peggy Guggenheim Collection (Venice), a multi-analytical approach involving Vis-NIR multispectral imaging, X-ray Fluorescence (XRF), External Reflectance Fourier Transform Infrared Spectroscopy (ER-FTIR), Raman spectroscopy, and Scanning Electron Microscopy coupled with energy dispersive X-ray analysis (SEM-EDS), was adopted to investigate several works of Max Ernst in the holding of the Peggy Guggenheim Collection.

Maximilian Maria Ernst (Brühl, 1891 - Paris, 1976), an influential artist of the early 20th century, was renowned for his embrace of unconventional imagery and an array of stylistic and technical innovations. His talent took shape under the influences of Expressionism and Dadaism, but over time he became one of the most representative artists of Surrealism Art, through which he developed a personal style. Notwithstanding Ernst's importance in art history, the technical studies on his materials and techniques are still very rare. To the authors' knowledge, there exist in the literature only few studies on Ernst's paintings [12-15]. This ongoing project aims at filling this gap, by investigating paintings by Ernst of different periods.

This paper reports on the study of the materials and the condition of the painting *Attirement of the Bride*. The artwork (Fig. 1), an oil on canvas painted in 1940, is one of Ernst's masterpieces. It is representative of his veristic or illusionistic Surrealism, whereby a traditional technique is applied to an anomalous and disturbing subject. An owl headed female figure, dressed with a splendid red robe that opens to reveal her body, dominates the picture. On the right is another female nude, while on the left a green large bird-man approaches [16]. In the upper left corner, the picture-within-a-picture presents the bride in the same pose, surrounded by a landscape of overgrown classical ruins. The splendour and elegance of the image contrasts with its primitivizing aspects - the loud colours, the zoomorphism - and the blunt phallic symbolism of the spearhead. Ernst had long identified himself with a bird and in 1929 had invented an alter ego, Loplop, Superior of the Birds. While the bride is generally thought to be the young English surrealist artist Leonora Carrington [17].



Fig. 1 *Attirement of the Bride* (129.6 × 96.3 cm), 1940. Courtesy of the Peggy Guggenheim Collection, Venice (The Solomon R. Guggenheim Foundation, New York), 76.2553 PG 78© Max Ernst, by SIAE 2008.

The painting is also the best example of Ernst's use of decalcomania, invented in 1935 by Oscar Domínguez. The technique involved diluted paint spread over some areas of the canvas and then covered and pressed on with a piece of glass or a sheet of paper [18].

The most visible use of decalcomania is in the picture-within-a-picture at the upper left of the painting. This rectangular surface was initially treated with decalcomania and, after drying, the sky and the nude female body were brushed in the contrasting, smooth and unified colour creating the spatial illusion of the figure-ground relationship. Decalcomania was also used to develop the marbled right edge of the main composition, the headdress of the otherwise nude female (right), and the feathered cloak of the central figure. In these areas, however, Ernst also used a combination of scumbling and elaborate minute brushstrokes to create veils of colour that, to varying degrees, obscure the decalcomania base. The nude bodies, the tiled floor and background, the green bird with a spear (left), and all other elements of the composition were brushed in afterwards, the outermost contours of the feathered forms being the last elements to be retouched [19].

Along with the figure of the bird, Ernst added lights and shadows with a small detailed brush. The colours consist of blue, white, yellow, and a different tone of green feathering. To further emphasize the contrast of light, the author painted along the arrow with a delicate hand in order to add smoothness. To create lustrous volume, Ernst used numerous colours to gain depth, shape and dimension. Along with small details, Ernst used two different motions of painting, rapid and fresh or slow and detailed. Finally, there is a deep red undertone over the direct painting clearly visible in the incisions of horizontal lines of the floor.

The painting was dated in the front part and signed on both front and reverse parts. Sometimes between 1964 and 1969 it was wax-lined [19] and other interventions were done in the same period including dusting, keying out of the canvas and addition of a new Plexiglas frame [20].

This paper shows the results of a non-invasive and limited micro-invasive analytical approach to the study of Ernst's painting materials, with a focus on the chemical composition of pigments and binders, as well as their alteration products.

3 Materials and methods

The *Attirement of the Bride* (129.6 × 96.3 cm) was analysed in situ in the PGC exhibition gallery. A preliminary analysis of the painting was performed by scanning the entire surface with Vis-NIR multispectral imaging. Information about the binder, composition of pigments and possible alteration products was provided by portable X-ray spectroscopy, Raman spectroscopy and ER-FTIR. The analysed points were chosen in order to obtain information about the global palette, selecting paints with different colours/hues. Twenty-eight points were analysed with XRF, 25 points with Raman spectroscopy and 11 points with ER-FTIR (Fig. S1 in Supplementary Materials). In addition, two

micro-samples were taken from the painting that spilled out on the canvas tacking edge. These cross-sections were analysed by a bench-top micro-Raman and SEM-EDS. The observed results were compared with those obtained with the non-invasive techniques adopted in situ.

The Multispectral Imaging system is equipped with a high-resolution Moravian G2-8300 camera (CCD detector KAF-8300, imaging area 18.1×13.7 mm, pixel size 5.4×5.4 μm) with a high dynamic range (16 bits). The sensor is cooled for reducing the electronic noise during the acquisition. The spectral resolution is obtained through the use of interferential filters with ± 25 nm pass bands around the central wavelengths: 450, 500, 550, 600, 650, in the visible range and 850, 950, 1050 nm in the near infrared.

In situ Raman measurements were performed with the portable instrument i-Raman® Plus, manufactured by BWTEK. It is equipped with a diode laser source emitting at 785 nm, the acquisition range goes from about 60 to 3300 cm^{-1} with a spectral resolution of ~ 3.5 cm^{-1} at 614 nm. The laser power in output from the optical fiber can vary from 0.3 up to 350 mW. Spectra were acquired with an exposure time of 10 s per acquisition and the laser power was set below of about 2.5 mW on the sample surface.

XRF experiments were carried out using the Elio portable XRF Analyzer (XGLab), equipped with a 10–40 keV/5–200 μA X-ray tube (Rh electrode, 1 mm collimated beam on the sample) and a large area Energy Dispersive Si-Drift detector (130 eV FWHM at Mn K).

Infrared spectra (ER-FTIR) were collected by means of an Alpha Bruker portable spectrometer equipped with an external reflection module, operating in the 7500–400 cm^{-1} range. Each spectrum was acquired with 160 scans and a resolution of 4 cm^{-1} . The investigated area is about 20 mm^2 . Due to the different contributions of surface and volume reflection, the absorptions are often affected by derivative-like distortion and/or band inversion. The heterogeneous nature of the substrate material – both chemical and physical – does not allow the use of Kramer-Kronig transform. Only a smoothing procedure was operated in post-production.

Polished cross-sections of two paint fragments were prepared by embedding them in a transparent polyester resin (Bascol, Colorchimica Spa): the cross-sections were firstly observed with an Olympus S2X12 stereomicroscope and then analysed with a bench-top micro-Raman and SEM-EDS.

A micro-Raman InVia instrument (Renishaw) was used equipped with a Leica microscope with a 50 \times objective, a diffraction grating with 1800 grooves/mm and a CCD detector. The measures were conducted in confocal mode in order to decrease the matrix signal, using two different lasers: HeNe ($\lambda = 633$ nm) and NdYag ($\lambda = 532$ nm).

SEM observations (FEI Quanta 200 FEG-ESEM, FEI Czech Republic s.r.o.) were carried out in high vacuum conditions, after metallization with carbon, and observed with two detectors: ETD (Everhart-Thornley Detector) and BSED (Back Scattered Electron Detector). Different magnifications were used according to the information to be acquired. The semi-quantitative elemental compositions and X-ray mapping were obtained by an Energy Dispersive X-ray Spectrometer EDAX Genesis, using an accelerating voltage of 20 keV.

4 Results and discussion

4.1 Preparatory drawing and *pentimenti*

The Vis-IR multispectral imaging (Fig. 2) reveals important information regarding the preparatory drawing and *pentimenti*. Fig. 2b shows the presence of prospective construction lines, such as an elliptic form on the figure on the right and a parallelepiped between the two female characters, which are not visible in the RGB image (Fig. 2a). In particular, it is interesting to note that the bottom line links the breasts of the two women, whereas the upper line crosses the eye of the bride. The perspective grid of the alternated white and black tiles on the floor was obtained by locating a vanishing point and building the orthogonal lines.

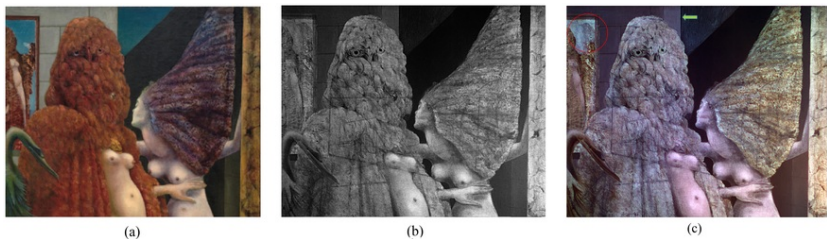


Fig. 2 VIS-NIR multispectral imaging, details of the painting in: (a) RGB, (b) IR (1050 nm) and (c) difference false colour merging (FC).

Fig. 2c reveals different *pentimenti*. In particular, it shows a reconsideration in the final phase of the painting of the length of the wall in the upper part of the painting (green arrow). In fact, in the RGB image (Fig. 2a) the wall is

longer than Fig. 2c, where a grey box is visible. Finally, the picture-within-a-picture (Fig. 2c, red circle) shows a figure which was covered during the painting process (Fig. 2a).

4.2 Materials identification

4.2.1 Ground layer, extenders and binder

Observing in detail the tacking margins of the canvas (Fig. S2 in Supplementary Materials), it is visible a lining of the original canvas on a restoration one and the presence of a white layer under the pictorial one can be hypothesized (Fig. S2b and S2e in Supplementary Materials). This theory is supported by non-invasive technique and, finally, confirmed by micro-invasive analyses performed on two micro-samples. XRF analysis shows the presence of S, Ba and Zn in all the analysed points; moreover, from the ER-FTIR spectra carried out in situ, we can infer the presence of barite (BaSO_4) in several points, on the basis of its overtone and combination bands. In fact, all the spectra show weak absorptions due to $\nu_1 + \nu_3$ ($\approx 2194\text{--}2137\text{--}2065\text{ cm}^{-1}$) and $2\nu_1$ ($\approx 1965\text{ cm}^{-1}$) of SO_4^{2-} group in barite (Fig. 3) [21]. Furthermore, ER-FTIR reveals also the presence of CaCO_3 , by showing in all the analysed areas a shoulder on the $\nu(\text{C}=\text{O})$ ester absorption, at $\approx 1796\text{ cm}^{-1}$, representative of the $\nu_1 + \nu_4$ combination bands and a weak absorption at $\approx 2512\text{ cm}^{-1}$ due to $\nu_1 + \nu_3$ of the CO_3^{2-} group (Fig. 3) [22].

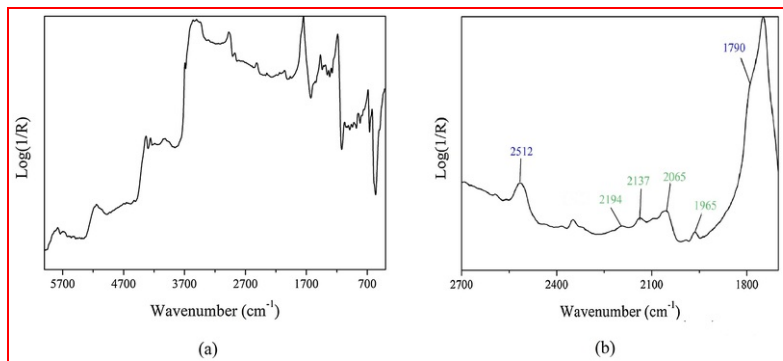


Fig. 3 ER-FTIR spectra of a flesh tone: (a) entire spectrum and (b) focus on BaSO_4 (green peaks) and CaCO_3 (blue peaks) detection region.

Therefore, on the basis of the information acquired with ER-FTIR and XRF, we can suppose the use of lithopone (barium sulphate + zinc sulphide, ZnS) as a white layer under the pictorial one. Moreover, the ubiquitous presence of the Pb lines in all the registered X-ray spectra could be attributed to the presence of lead white, $2\text{PbCO}_3 \cdot \text{Pb}(\text{OH})_2$, as a second type of ground layer or underpainting. In fact, the use of lead white is well documented, alone or in combination with other white pigments or, in commercial white grounds, with extenders [23]. Indeed, its use as a white pigment by Max Ernst is also reported in a study by A. King et al. [13].

The absence of lead white or lithopone in certain sampling points analysed with ER-FTIR and in situ Raman analyses could be attributed to a precise choice of the artist or to his painting technique (e.g. the decalcomania) leading to an uneven distribution of the underpainting. Besides, the higher penetration of X-rays can explain why these pigments are not or barely detected by ER-FTIR and in situ Raman spectroscopy directly on the painting. Moreover, in order to prevent possible damages on the canvas, the laser power of the Raman spectrometer was set to a few milliwatt ($< 3\text{ mW}$). Unfortunately, this low power does not allow a penetration to the ground layer.

To confirm the hypothesis of the presence of the white ground layer, SEM-EDS and micro-Raman analysis were performed on the cross-section obtained from two micro-samples taken from the painting. Sample 1 corresponds to a white layer (Fig. 4a), while sample 2 is composed by a white and a blue layer (Fig. 5a). Furthermore, also a red shade is present at the interface between the two layers. The results show that these samples are representative, confirming some of the findings obtained with non-invasive techniques. X-ray maps performed on sample 1 (Fig. 4c) reveal that barium and lead are uniformly distributed in the layer. Zinc is also present, but to a lesser extent than barium and lead.

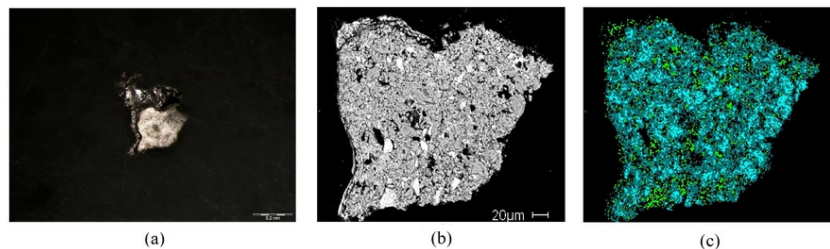


Fig. 4 Cross-section of sample 1: (a) OM Image (90 \times), (b) BSE image and (c) Ba (L line) distribution in green and Pb (L line) distribution in cyan.

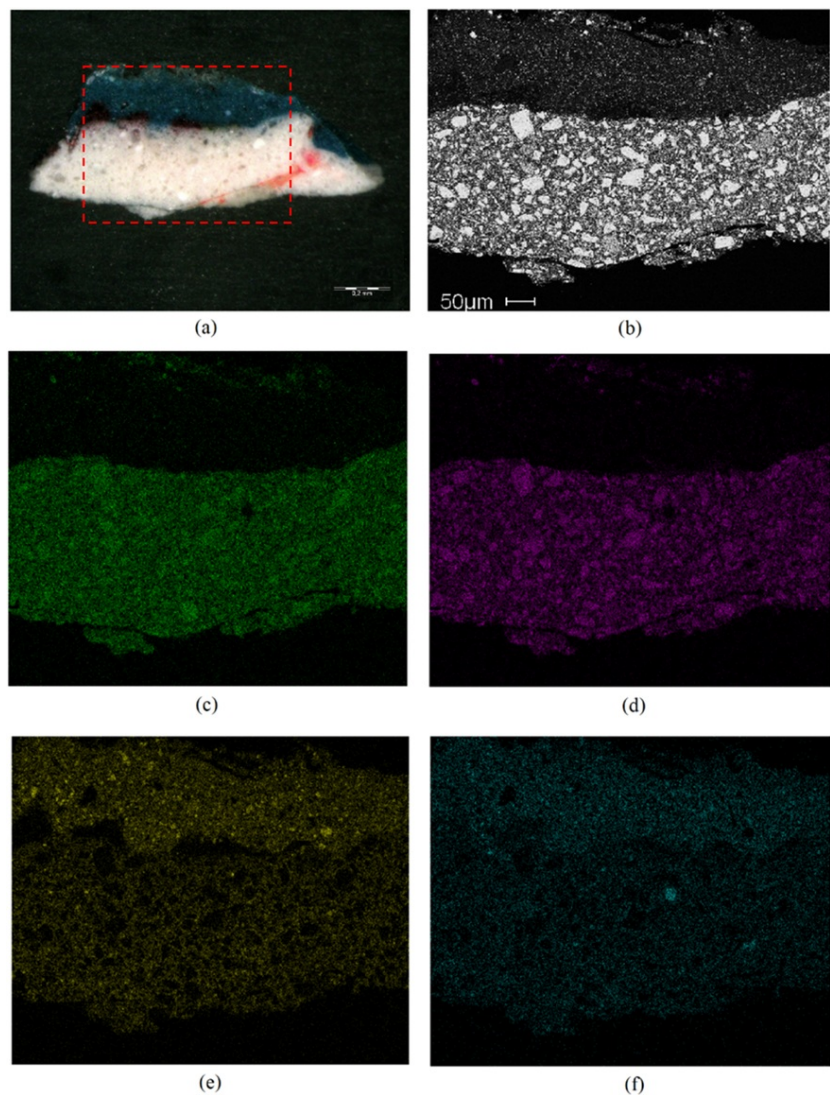


Fig. 5 Cross-section of sample 2: (a) OM Image (90 \times), the red dotted rectangle circumscribes the SEM mapped area, (b) BSE image, (c) S (K line) distribution, (d) Ba (L line) distribution, (e) Ca (K line) distribution and (f) Zn (K line) distribution.

The micro-Raman analysis confirms these data by showing lead white, with a characteristic absorption peak at 681 cm^{-1} (C-O rocking deformation in CO_3 group) and 1050 cm^{-1} (C-O symmetric stretching in CO_3 group) [24], in addition to lithopone (main bands at 347 cm^{-1} referred to ZnS, and $450, 984\text{ cm}^{-1}$ referred to BaSO_4) [25,26] supporting the previous results and the possibility of its use in the ground layer.

The elemental distribution obtained by sample 2 (Fig. 5) highlights that S and Ba (Fig. 5c and d, respectively) are mainly concentrated on the ground layer. Instead, Ca and Zn (Fig. 5e and f, respectively) are distributed over the entire section, most likely in the pictorial layer. The compresence of Ba, Zn and S in the white layer confirms the use of lithopone, as suggested by micro-Raman analysis with main absorption bands at $347, 450$ and 984 cm^{-1} [26]. Concerning Ca, the high amount of Ca in both white ground layer and pictorial one could be associated to the presence of calcium carbonate, identified also by micro-Raman technique with main bands at 710 and 1083 cm^{-1} (symmetric bending and symmetric stretching of CO_3 group, respectively) [26,27] and previously confirmed by ER-FTIR. From its distribution, we can suppose that CaCO_3 is probably used both mixed with lithopone in the ground and in the pictorial layer. In the latter case, it could be used as a white pigment or it could be present

in the paint tube as an extender.

The presence of Zn in the pictorial layer could be due to the ZnS present in the lithopone, which migrates to the top of the white ground layer, and/or also to zinc carboxylates.

Regarding the presence of this ground layer under the pictorial one, it is most likely a commercial preparatory coating applied by the producer of the canvas; indeed, [the conservation report of examination \(1985\) of *The Antipope* a document referred to the *Antipope*](#) (another Ernst's masterpiece performed in 1942) reports the presence of a commercially primed canvas [28].

The use of a siccative oil, probably linseed, can be inferred by the presence of a strong absorption centred at $\approx 1740\text{ cm}^{-1}$ together with two weak peaks at ≈ 4340 and 4260 cm^{-1} . The former is representative of the asymmetric $\nu(\text{C}=\text{O})$ ester, while the latter is due to the combination of the stretching and bending bands ($\nu_a + \delta_a$ and $\nu_s + \delta_s$ respectively) of the aliphatic methylene units in linseed oil [29,30] (Fig. S3 in Supplementary Materials). It is worthy to observe that the use of a siccative oil is also supported by the absence of the typical signal of an alkyd resin (4670 cm^{-1} and 1270 cm^{-1}).

4.2.2 Palette

Regarding the pigments, the analysed points are organized in accordance to the main types of colour.

4.2.2.1 Black The analysed black paint reveals the presence of amorphous carbon with characteristic absorption peak at 1590 cm^{-1} and a broad peak at around 1300 cm^{-1} showed by Raman technique[25,31].

4.2.2.2 Blue For all the analysed points, in situ Raman technique reveals the presence of phthalocyanine blue $\text{CuC}_{32}\text{H}_{16}\text{N}_8$. The signals at 680 and 748 cm^{-1} are due to the breathing and deformation vibration of the macrocycle [22]. The main intense signal at 1527 cm^{-1} corresponds to the principal macrocycle stretching vibration [32], and the band at 1341 cm^{-1} is due to the C-C stretching [22,33] (Fig. 6). This result is also confirmed by μ micro-Raman performed on the blue part of sample 2 (Fig. S4 in Supplementary Materials). This is a very interesting finding because phthalocyanine blue is a new pigment, discovered in 1907 [34] but commercialized as monastral fast blue only in the 1930s [35]. Furthermore, Prussian blue, a ferric hexacyanoferrate, was used by the artist to create several shades in violet, yellow, green and flesh tones. This pigment was recognized thanks to characteristic Raman absorption peaks at 2097 and 2152 cm^{-1} both referred to the stretching vibration of C

N group [36]. Furthermore, also XRF technique shows the presence of Fe in the analysed points.

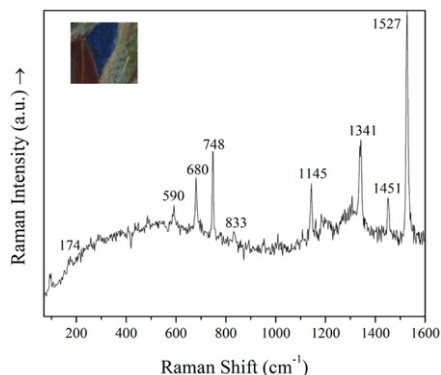


Fig. 6 In situ Raman spectrum of a blue tone that identifies phthalocyanine blue.

4.2.2.3 Red Two types of red paints can be recognized on the painting: a more orange-red tone and a more intense one. For the first type, in situ Raman technique identifies iron oxide (Fe_2O_3) with the characteristic peak at 225 and 291 cm^{-1} associate to Fe-O symmetric bending [37], lithopone and lead white. XRF analysis confirms these data showing the presence of Fe, Pb, Ba, Zn and S.

Regarding the presence of iron oxide, XRF analysis performed in situ reveals the presence of Fe in several analysed points, ~~and Fe~~ furthermore, as reported in the introduction, there is a red undertone in the incisions of horizontal lines of the floor. However, it is difficult to say if this compound is homogeneously present under the paint layer or if it is used only in some points to have some particular effect.

In the intense red tones, Raman spectroscopy identifies an azo β -naphthol pigment, with characteristic absorption peaks at 1328 , 1397 and 1447 cm^{-1} [26] mixed with lead white and lithopone.

In this case, the lead white could have been chosen as a pigment or it could be referred to the white ground layer: the fact that ~~it~~ is visible with Raman analysis could be due to the ~~D~~decalcomania technique which leads to uneven distribution of the underpainting layer.

The results showed by in situ techniques are confirmed by the **micro**-Raman analyses performed on the red paint at the interface of the blue and white region of the sample 2 (Fig. 5a). This tone results composed of iron oxide (Fig. S5a in Supplementary Materials), an azo β -naphthol pigment (Fig. S5b in Supplementary Materials) and lithopone (Fig. S5a and S5b in Supplementary Materials).

4.2.2.4 Violet The violet paints (Fig. 7) result as a mixture of Prussian blue and iron oxide, with additions of lithopone and calcium carbonate, probably to give a lighter shade. Lithopone was identified with characteristic Raman peaks at 452, 460, 61 and 987 cm^{-1} and CaCO_3 with the main peak at 1086 cm^{-1} [26]. Furthermore, XRF analysis shows the presence of Co in all the points, suggesting the presence of a **Cocobalt**-based pigment.

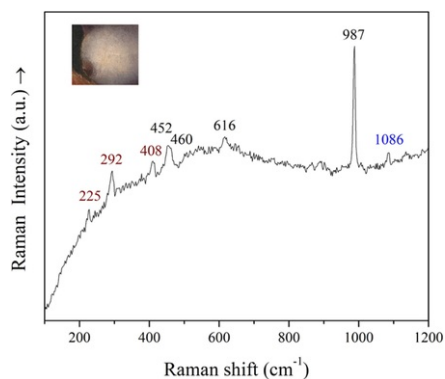


Fig. 7 In situ Raman spectrum of a violet paint identifying iron oxide (red peaks), lithopone (black peaks) and calcium carbonate (blue peak).

4.2.2.5 Yellow Raman analysis of yellow tones shows the presence of barium chromate also known as lemon yellow (BaCrO_4) with a characteristic absorption peak at 864 cm^{-1} which refers to the chromate stretching mode [26,38], CaCO_3 and lithopone (Fig. S6 in Supplementary Materials). The presence of BaCrO_4 is confirmed by XRF analysis which identifies the presence of Ba and Cr. The ER-FTIR fingerprint region does not allow a straightforward identification of the CrO_4^{2-} stretching mode in lemon yellow because of the overlap of the spectral contributions from different compounds in the pictorial layer.

The ER-FTIR spectrum clearly shows two weak signals attributable to silicates, probably kaolin (Fig. S7 in Supplementary Materials). The former, centred at 3695 cm^{-1} , is associated to the stretching of the hydroxyl group in silicate structure, while the latter, at 4523 cm^{-1} , is related to the $\nu + \delta$ (OH) combination band [21]. Moreover, an intense inverted band, at $\approx 545 \text{ cm}^{-1}$, could be referred to both the bending modes in silicate structure, i.e. δ (SiO), δ (AlO), and/or to the stretching mode in iron oxide/oxyhydroxide [39]. Taking into account the presence of Fe, detected by XRF, the use of a yellow ochre can be inferred.

4.2.2.6 Green All the green paints seem to be obtained by the mixtures of blue and yellow pigments, rather than derived from a single green pigment. In fact, Raman spectra show the presence of Prussian blue, while XRF analysis identifies Cr and Ba. Due to this evidence, we can suppose a mixture of Prussian blue and barium chromate (which was identified also for the yellow areas). Unfortunately, Raman spectra gave no evidences of the presence of barium chromate since the obtained spectra were very noisy. However, the presence of Ba and Cr in XRF spectra supports our hypothesis.

Furthermore, XRF technique evidences the presence of Co in some of the green points. Therefore, we can infer the presence of a **Cocobalt**-based pigment.

4.2.2.7 Brown Raman technique identifies iron oxide (225, 291 and 609 cm^{-1}), while XRF shows the presence of Fe and Mn. Therefore, this tone is probably obtained with a raw umber (Fig. 8).

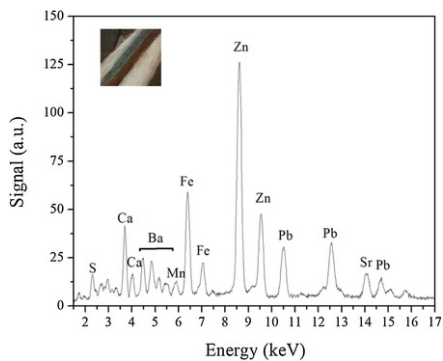


Fig. 8 XRF representative spectrum of a brown paint.

4.2.2.8 White Raman analysis on white paints shows the presence of titanium dioxide in its anatase form with characteristic absorption peaks at 144 and 637 cm^{-1} due to the symmetric stretching vibration of O-Ti-O, 395 cm^{-1} referred to the symmetric bending vibration of O-Ti-O and 516 cm^{-1} due to the antisymmetric bending vibration of O-Ti-O [40]. Lithopone and CaCO_3 are also detected (Fig. 9).

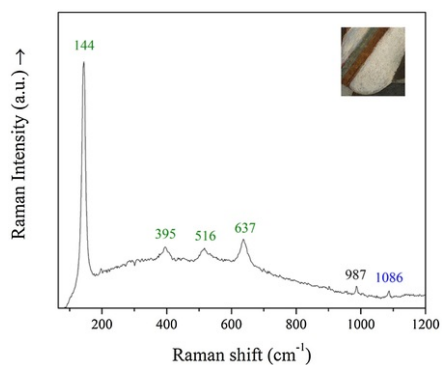


Fig. 9 In situ Raman spectrum of a white paint identifying anatase (green peaks), lithopone (black peak) and calcium carbonate (blue peak).

4.2.2.9 Flesh All the flesh tones are obtained with a mixture of several pigments. In fact, the based colour is probably due to a mixture of lithopone and/or CaCO_3 , silicates (recognized by ER-FTIR analysis), iron oxide (showed by Raman technique) and a raw umber (suggested by the presence of Mn showed by XRF analysis, Fig. 10). Different hues are then obtained by varying pigments. In fact, Raman technique shows the presence of Prussian blue in some points; instead, XRF analysis reveals the presence of Co which can be related to a cobalt-based pigment (Fig. 10). From these findings, we can state that Ernst used a variety of pigments and combinations with basic lithopone, calcium carbonate and umbers; to give different hues to the flesh tones, he used mainly Prussian blue.

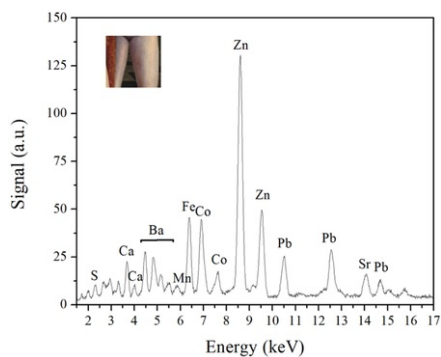


Fig. 10 XRF spectrum of a flesh tone.

4.2.2.103 Alteration products and retouching The study of the ER-FTIR spectra allows some considerations on the state of condition and the presence of retouching. In fact, in all the analysed areas, the carbonyl ester stretchin exhibits a partial derivative distortion ($\approx 1740\text{ cm}^{-1}$) more broadened towards low wavenumbers. Such broadening could be ascribed to the superimposition of different contributions such as the photo-oxidative degradation of siccative oils [41], the presenc of alteration products and/or the presence of organic materials as a consequence of restoration interventions.

Signals attributable to metal soaps and/or oxalates were also detected on the whole canvas (Fig. 11). While the former can be also present as additives in the paint formulation [42], the latter are significant, suggesting alteration processes in the paint layer [43,44]. In fact, metal soaps, e.g. stearates, show distinctive absorptions between 1600 and 1400 cm^{-1} [45] (Fig. 11c). The presence of a Zn carboxylate can be inferred by the weak derivative $\nu_a(\text{COO}^-)$ band at 1541 cm^{-1} [30] (Fig. 11c). This weak signal is noticeable especially on the flesh tones, but also in the yellow, blue and green areas. Moving to metal oxalates, excluding the blue area, $\text{ZnC}_2\text{O}_4 \cdot 2\text{H}_2\text{O}$ can be tentatively supposed by the distinctive doublet at ≈ 1364 and $\approx 1320\text{ cm}^{-1}$, ascribable to the $\nu_s(\text{COO}^-)$ [46] (Fig. 11c). In addition, metal oxalates show also distinctive $\nu(\text{OH})$ derivative shaped bands between 3500 and 3300 cm^{-1} [46] (Fig. 11a). Moreover, some areas show a significant inflection at 1640 cm^{-1} on the $\nu(\text{C}=\text{O})$ ester absorption (Fig. 11c). This signal, tentatively attributed to the asymmetric stretching of CO group in $\text{ZnC}_2\text{O}_4 \cdot 2\text{H}_2\text{O}$, supports the presence of such alteration product [46].

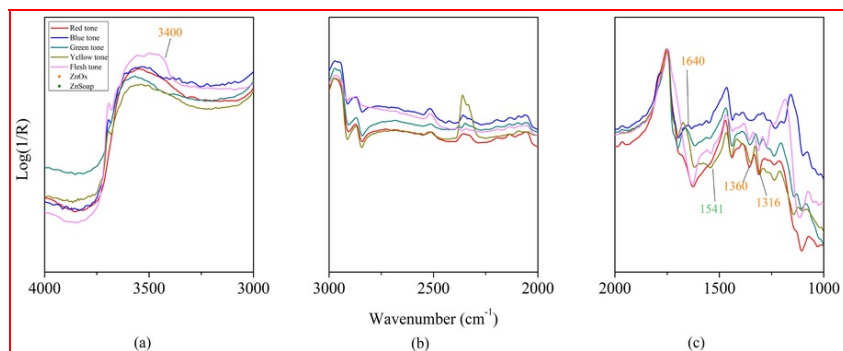


Fig. 11 ER-FTIR absorption bands of zinc oxalates (orange peaks) and zinc metal soaps (green peaks) found in the different tones.

5 Conclusions

This study revealed that a multi-analytical approach is suitable for the identification of the painting materials used in modern oil paintings. The results revealed that the *Attirement of the Bride* shows a preparatory layer, probably already present in the commercial canvas, on which the artist painted by using a limited range of mostly traditional pigments, sometimes related to new industrial production. In fact, the palette includes not only quality tube paints (without extenders) but also commercial, sometimes recent, paints.

The preparatory layer consists of lithopone, lead white and calcium carbonate. This latter compound is also present in different areas, added to other pigments. Therefore, it could have been used intentionally as a white pigment or, in some cases, already be present in the paint tube as an extender.

The palette shows the presence of primary colours as phthalocyanine blue, barium chromate, lithopone, iron oxide, anatase and β -naphthol. Prussian blue was used only to give specific shades in violet, yellow, green and flesh tones. Cobalt-based pigments were also added in some areas to create different shades.

Although the range of paints is limited, Ernst showed a great awareness of their possibilities by using, for instance, phthalocyanine blue when a definite blue colour was needed and Prussian blue only to create other colours or hues. However, since the painting was created at the beginning of the World War II, we cannot be sure if he made a conscious choice of materials or if he was forced to use some particular pigments due to the difficult condition in which he was working.

His mastery of the pictorial technique is also confirmed by both the imaging results which indicate a planning of the painting (even if some *pentimenti* can also be seen), and the use of decalcomania. This is in line with what was found in a study on his works of the early 1920s performed at the Tate Gallery Britain (I changed three figures in supplementary materials: only formal changes were applied.) [13].

The occurrence of a degradation process has been evidenced by the presence of zinc oxalates and zinc metal soaps. However, it is difficult to confirm if zinc metal soaps were present as additives in the paint tubes or if they formed subsequently as alteration products.

Acknowledgments

This study has been performed thanks to the project “TORNO SUBITO 2017” Programma di interventi rivolto agli student universitari e laureati. It has been in part supported by MIUR (PRIN 2015 - 2015WBEP3H). We would like to thank Karole Vail, Director of the Peggy Guggenheim Collection (Venice) for allowing the analysis on the painting and Mr Siro De Boni for the practical support during the investigation at the museum. The museum is acknowledged for providing the high-resolution image of the painting. We also wish to thanks Chiara Barbieri, director of publications and special projects.

Appendix A. Supplementary data

Supplementary material related to this article can be found, in the online version, at <http://dx.doi.org/10.1016/j.culher.2019.10.010>.

References

- [1] T. Learner, Analysis of modern paints, 2004, The getty conservation institute.
- [2] O. Chiantore and A. Rava, Conservare l'arte contemporanea: problemi, metodi, materiali, ricerche, 2005, Mondadori Electa; Milano.
- [3] K. Van den Berg and A. Burnstock, Twentieth century oil paint. The Interface Between Science and Conservation and the Challenges for Modern Oil Paint Research, In: G.H.K. Jan van den Berg, A. Burnstock, M. de Keijzer, J. KruegerKlaas, T. Learner and A. de Tagle, (Eds.), *Issues in contemporary oil paint*, 2015, Springer, 1-19.
- [4] M. Doerner, The materials of artists and their use in painting, 1984, Harvest; San Diego/New York/London.
- [5] R. Mayer, The artist's handbook of materials and techniques, Revisited, 1991, Viking; New York.
- [6] F.C. Izzo, K.J. Van Den Berg, H. Van Keulen, B. Ferriani and E. Zendri, Modern Oil Paints - Formulations, Organic Additives and Degradation: Some Case Studies, In: G.H.K. Jan van den Berg, A. Burnstock, M. de Keijzer, J. KruegerKlaas, T. Learner and A. de Tagle, (Eds.), *Issues in Contemporary Oil Paint*, 2015, Springer, 75-104.
- [7] A. Daveri, S. Piazani, M. Marmion, H. Harju and A. Vidman, New perspectives in the non-invasive, in situ identification of painting materials: The advanced MWIR hyperspectral imaging, *Trends Anal. Chem.* **98**, 2018, 143-148.
- [8] A. Martins, C. Albertson, C. McGlinchey and J. Dik, Piet Mondrian's Broadway Boogie Woogie: non invasive analysis using macro X-ray fluorescence mapping (MA-XRF) and multivariate curve resolution-alternating least square (MCR-ALS), *Herit. Sci.* 2016, 1-16.
- [9] S. Steger, H. Stege, S. Bretz and O. Hahn, A complementary spectroscopic approach for the non-invasive in-situ identification of synthetic organic pigments in modern reverse paintings on glass (1913-1946), *J. Cult. Herit.* **38**, 2019, 20-28.
- [10] A. Nevin and T. Doherty, The Noninvasive analysis of Painted Surfaces, Scientific impact and Conservation Practise, In: S.I.S. Press, (Ed), *Smithsonian contributions to museum conservation, number 5*, 2016, Smithsonian

Institution Scholarly Press; Washington DC.

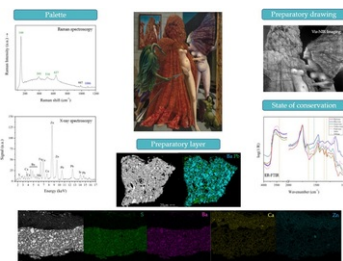
- [11] L. Rampazzi, V. Brunello, C. Corti and E. Lissoni, Non-invasive techniques for revealing the palette of the Romantic painter Francesco Hayez, *Spectrochim. Acta Part A Mol. Biomol. Spectrosc.* **vol. 176**, 2017, 142-154.
- [12] J. Coddington and S. Siano, Studies in Conservation Infrared imaging of twentieth-century works of art, *Stud. Conserv.* **45** (suppl. 1), 2000, 39-44.
- [13] A. King, J. Townsend and A. Wright, Max Ernst's painting processes in the early 1920s, In: A. King, J. Townsend and A. Wright, (Eds.), *Picasso, Picabia, Ernst: New Perspectives*, 2018, Archetype; London, 123-135.
- [14] E. Hanspach-Bernal and A. Bezúr, Adding and removing: two Surrealist paintings by Max Ernst from the Menil Collection, Houston, In: A. King, J. Townsend and A. Wright, (Eds.), *Picasso, Picabia, Ernst: New Perspectives*, 2018, Archetype; London, 136-140.
- [15] E. Hanspach-Bernal and A. Bezúr, Between chance and choice: Max Ernst's frottages and grattages on canvas from the Menil Collection, Houston, In: C. Krekel, J.H. Townsend, S. Eyb-Green, K. Pilz and J. Kirby, (Eds.), *Expression and Sensibility: Art Technological Research*, 2018, Archetype; London, 81-87.
- [16] F. Rosemont and M.E. Warlick, *Max Ernst and Alchemy: A Magician in Search of Myth*, 2001, University of Texas Press.
- [17] The Peggy Guggenheim Collection. [Online]. Available: <http://www.guggenheim-venice.it>.
- [18] W. Spies, I. Müller-Westermann, K. Degel, J. Drost and T. Wessolowski, *Max Ernst: Dream and Revolution*, 2009, Louisiana Museum of modern art.
- [19] A.Z. Rudenstine, *Peggy Guggenheim Collection*, 1985, Venice.
- [20] A. Michieletto, *Ernst PG 71 Conservation Treatment*. p. 1981.
- [21] C. Miliani, F. Rosi, A. Daveri and B.G. Brunetti, Reflection infrared spectroscopy for the non-invasive in situ study of artists' pigments, *Appl. Phys. A* **106**, 2012, 295-307.
- [22] M. Vagnini, F. Gabrieli, A. Daveri and D. Sali, Handheld new technology Raman and portable FT-IR spectrometers as complementary tools for the in situ identification of organic materials in modern art, *Spectrochim. Acta Part A Mol. Biomol. Spectrosc.* **176**, 2017, 174-182.
- [23] A. Roy, *Artists' Pigments, A Handbook of Their History and Characteristics, Volume 2*, 1993, National Gallery of Art, Washington Archetype Publications; London.
- [24] D. Goltz, J. McClelland, A. Schellenberg, M. Attas, E. Cloutis and C. Collins, Spectroscopic Studies on the Darkening of Lead White, *Appl. Spectrosc.* **57** (11), 2003, 1393-1398.
- [25] V. Košarova, D. Hradil, J. Hradilová, Z. Čermáková, I. Němec and M. Schreiner, The efficiency of micro-Raman spectroscopy in the analysis of complicated mixtures in modern paints: Munch's and Kupka's paintings under study, *Spectrochim. Acta Part A Mol. Biomol. Spectrosc.* **156**, 2016, 36-46.
- [26] L. Burgio and R.J.H. Clark, Library of FT-Raman spectra of pigments, minerals, pigment media and varnishes, and supplement to existing library of Raman spectra of pigments with visible excitation, *Spectrochim. Acta Part A Mol. Biomol. Spectrosc.* **57** (7), 2001, 1491-1521.
- [27] S. Gunasekaran, G. Anbalagan and S. Pandi, Raman and infrared spectra of carbonates of calcite structure, *J. Raman Spectrosc.* **37** (9), 2006, 892-899.
- [28] E. Estabrook, *The Peggy Guggenheim collection conservation report of examination*. 1965.
- [29] F. Rosi, A. Daveri, P. Moretti, B.G. Brunetti and C. Miliani, Interpretation of mid and near-infrared reflection properties of synthetic polymer paints for the non-invasive assessment of binding media in twentieth-century pictorial artworks, *Microchem. J.* **124**, 2016, 898-908.
- [30] F. Rosi, et al., Disclosing Jackson Pollock's palette in Alchemy (1947) by non-invasive spectroscopies, *Herit. Sci.* **4** (18), 2016, 1-13.
- [31] E.P. Tomasini, E.B. Halac, M. Reinoso, E.J. Di Liscia and M.S. Maier, Micro-Raman spectroscopy of carbon-based black pigments, *J. Raman Spectrosc.* **43**, 2012, 1671-1675.
- [32] C. Defeyt, P. Vandenebeele, B. Gilbert, J. Ven Pevenage, R. Cloots and D. Strivay, Contribution to the identification of α -, β - and ϵ -copper phthalocyanine blue pigments in modern artists' paints by X-ray powder diffraction, attenuated total reflectance micro-fourier transform infrared spectroscopy and micro-Raman spectroscopy, *J. Raman Spectrosc.* **43**, 2012, 1772-1780.

- [33] J. Jiang, L. Rintoul and D.P. Arnold, Raman spectroscopic characteristics of phthalocyanine and naphthalocyanine in sandwich-type (na)phthalocyaninato and porphyrinato rare earth complexes, *Polyhedron* **19**, 2000, 1381-1394.
- [34] M. de Keijzer, The Delight of Modern Organic Pigment Creations, In: G.H.K. Jan van den Berg, A. Burnstock, M. de Keijzer, J. KruegerKlaas, T. Learner and A. de Tagle, (Eds.), *Issues in Contemporary Oil Paint*, 2015, Springer: 44-73.
- [35] G. Poldi and S. Caglio, Phthalocyanine Identification in Paintings by Reflectance Spectroscopy. A Laboratory and In Situ Study, *Opt. Spectrosc.* **114** (6), 2013, 929-935.
- [36] R. Chen, Q. Zhang, Y. Gu, L. Tang, C. Li and Z. Zhang, One-pot green synthesis of Prussian blue nanocubes decorated reduced graphene oxide using mushroom extract for efficient 4-nitrophenol reduction, *ACA* **853**, 2015, 579-587.
- [37] A. Needham, et al., The application of micro-Raman for the analysis of ochre artefacts from Mesolithic palaeo-lake Flixton, *J. Archaeol. Sci. Reports* **17**, 2018, 650-656.
- [38] A. Giakoumaki, I. Osticioli and D. Anglois, Spectroscopic analysis using a hybrid LIBS-Raman system, *Appl. Phys. A* **83**, 2006, 537-541.
- [39] C. Germinario, et al., Multi-analytical and non-invasive characterization of the polychromy of wall paintings at the Domus of Octavius Quartio in Pompeii, *Eur. Phys. J. Plus* **133** (9), 2018.
- [40] R.M. Tamgadge and A. Shukla, Electrochimica Acta Fluorine-doped anatase for improved supercapacitor electrode, *Electrochim. Acta* **289**, 2018, 342-353.
- [41] M. Lazzari and O. Chiantore, Drying and oxidative degradation of linseed oil, *Polym. Degrad. Stab.* **65** (2), 1999, 303-313.
- [42] G. Osmond, Zinc Soaps: An Overview of Zinc Oxide Reactivity and Consequences of Soap Formation in Oil-Based Paintings, in: F. Casadio, K. Keune, P.N.A. Van Loon, E. Hendriks, S.A. Centeno, G. Osmond (Eds.), *Metal soaps in art Conservation and Research*, 2019, pp. 25-47.
- [43] F. Rosi et al. Tracking Metal Oxalates and Carboxylates on Painting Surfaces by Non-invasive Reflection Mid-FTIR Spectroscopy, in: F. Casadio, K. Keune, P.N.A. Van Loon, E. Hendriks, S.A. Centeno G. Osmond (Eds.), *Metal soaps in art Conservation and research*, 2019, pp. 173-195.
- [44] J. La Nasa, A.L. Tenorio, F. Modugno and I. Bonaduce, Two-step analytical procedure for the characterization and quantification of metal soaps and resinates in paint samples, *Herit. Sci.* **6** (57), 2018, 1-10.
- [45] V. Otero, et al., Characterisation of metal carboxylates by Raman and infrared spectroscopy in works of art, *J. Raman Spectrosc.* **45** (July), 2014, 1197-1206.
- [46] L. Monico, F. Rosi, C. Miliani, A. Daveri and B.G. Brunetti, Non-invasive identification of metal-oxalate complexes on polychrome artwork surfaces by reflection mid-infrared spectroscopy, *Spectrochim. Acta Part A Mol. Biomol. Spectrosc.* **116**, 2013, 270-280.

Appendix A. Supplementary data

[Multimedia Component 1](#)

Graphical abstract



Highlights

- A multi-technique approach has been used to study Max Ernst's masterpiece.
- Vis-NIR imaging revealed a preparatory drawing and *pentimenti*.
- Conscious use of colour palette which includes both traditional and synthetic pigments.
- ER-FTIR analysis evidenced Zn oxalates and Zn metal soaps as degradation products.

Queries and Answers

Query: The author names have been tagged as given names and surnames (surnames are highlighted in teal color). Please confirm if they have been identified correctly.

Answer: Yes

Query: Have we correctly interpreted the following funding source(s) and country names you cited in your article:MIUR?

Answer: Yes